VIRTUAL PULSE DESIGN FOR IEEE 802.11AD-BASED JOINT COMMUNICATION-RADAR

Preeti Kumari[1], *Sergiy A. Vorobyov*[2], *and Robert W. Heath, Jr.*[1]

[1] The University of Texas at Austin, TX, USA, email: {preeti_kumari, rheath}@utexas.edu
[2] Aalto University, Espoo, Finland, email: sergiy.vorobyov@aalto.fi

ABSTRACT

The millimeter wave WLAN standard can be used for joint communication-radar by exploiting the waveform preamble as a radar pulse. The velocity estimation accuracy with this approach, however, is limited due to the short integration time. A physical increase in the radar pulse integration duration, however, leads to a decrease in the communication data rate. In this paper, a coprime-based pulse design approach for IEEE 802.11ad-based radar is proposed that uses only a few non-uniformly placed preambles to construct several virtual pulses for enhancing the velocity estimation accuracy/resolution as compared to the conventional approach without sacrificing the communication data rate. The simulation results demonstrate that the coprime-based virtual pulse design improves the velocity estimation resolution by a factor of about 60x at a vehicle separation distance of 10 m and by a factor of about 20x at a distance of 100 m, while simultaneously achieving 7 Gbps data rate.

1. INTRODUCTION

A joint communication-radar system with hardware reuse has significant advantages in terms of cost, size, spectrum usage, and adoption of communication-capable vehicles. Unfortunately, most of the proposed joint systems operate at sub-6 GHz bands. As a result, they suffer from poor radar resolution and low communication rates [1]. In [2], a joint mmWave vehicular communication-radar system based on the IEEE 802.11ad single-carrier physical layer (SC PHY) modulation was proposed. Although [2] simultaneously achieved a cm-level range resolution and a Gbps data rate by exploiting the preamble of a single frame for radar, the velocity estimation performance was limited. To enhance the velocity estimation resolution without any modification of the IEEE 802.11ad SC PHY frame structure, [3] investigated the possibility of increasing the radar integration duration by using multiple fixed length frames. This approach, however, needs a large physical increase in the total preamble duration for achieving high velocity estimation performance, which would incur a significant degradation in the communication data rate.

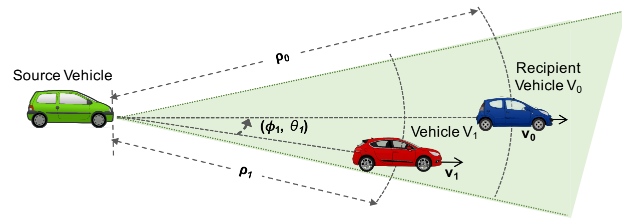

Fig. 1. The source vehicle sends an adaptive IEEE 802.11ad waveform to the recipient vehicle receiver and uses the echoes from surrounding vehicles to estimate their ranges/velocities.

In this paper, we propose a virtual pulse design approach for an adaptive joint communication-radar system based on the SC PHY frame of the IEEE 802.11ad standard. In this approach, the frame lengths are varied such that their preambles, which are exploited as radar pulses, are placed in a coprime fashion. A few non-uniformly placed pulses in a coherent processing interval (CPI) are then used to construct a virtual block with several pulses, leveraging the sparsity inherent in the mmWave channel. This virtually increases the radar pulse integration time and enables an enhanced velocity estimation performance, a more flexible waveform design, and a relaxed trade-off with the communication rate as compared to [3]. Numerical simulations demonstrate that the coprime-based approach leads to a cm/s-level velocity resolution in a 1 ms CPI, which meets the required velocity performance in automotive radars [4], with significantly lower communication rate-distortion as compared to the uniform approach.

2. SYSTEM MODEL

Consider a joint communication-radar system, where a source vehicle communicates with a recipient vehicle V_0 while simultaneously sensing surrounding targets, as shown in Fig. 1.

Transmit Signal Model: Consider a CPI of T seconds occupying M frames. During the CPI, the relative acceleration and velocity of a target/recipient vehicle with respect to the source vehicle are small enough such that the constant velocity and quasi-stationarity (constant location parameters) assumptions hold. The complex baseband continuous-time

This research was supported by the U.S. Department of Transportation through the Data-Supported Transportation Operations and Planning (D-STOP) Tier 1 University Transportation Center and by the Texas Department of Transportation under Project 0-6877 entitled "Communications and Radar-Supported Transportation Operations and Planning (CAR-STOP)".

representation of m^{th} transmit (TX) frame consisting of N_m symbols with T_{s} sample duration is

$$x_m(t) = \sum_{n=0}^{N_m-1} s_m[n] g(t - nT_{\text{s}}) \tag{1}$$

where n is the symbol index in m^{th} frame, $s_m[n]$ is the TX symbol sequence corresponding to m^{th} adaptive IEEE 802.11ad SC PHY frame with $\mathbb{E}\left[|s_m[n]|^2\right] = \mathcal{E}_{\text{s}}$, and $g(t)$ is the unit energy pulse-shaping filter.

Since IEEE 802.11ad supports a single data stream, we use adaptive analog beamforming with large phased array TX/receive (RX) antennas for the proposed mmWave system to achieve highly directional beamforming towards the communication RX. We consider a full-duplex radar assumption at the source vehicle due to the recent development of systems with sufficient isolation and self-interference cancellation [5,6]. To explore the trade-off between communication data rate and radar velocity estimation resolution, we consider an illustrative example of a single-target vehicle scenario. Assuming there is no blockage between the source and target vehicles, the highly directional mmWave communication link is established with the line-of-sight (LoS) radar and communication channels [7]. For simplicity and due to the space limitation, the LoS radar channel is assumed to be frequency-flat, as in [3, 8], where the recipient vehicle with range ρ_0 and velocity v_0 is the only dominant direct path target scatter. Analogous to the radar channel, the LoS mmWave communication channel is assumed to be narrowband [9]. The approach and insights developed in this paper can be extended to a multi-target scenario by including frequency-selective channel models [10]. After TX/RX beamforming, matched filtering, symbol rate sampling, the communication/radar RX signal model in a CPI can be formulated as follows.

Communication Received Signal Model: After time and frequency synchronization, the discrete-time received communication signal at the recipient vehicle corresponding to n^{th} symbol in m^{th} frame is given as

$$y_{\text{C}}[m,n] = h_{\text{C}} s_m[n] + z_{\text{C}}[m,n] \tag{2}$$

where h_{C} is the complex one-way communication channel gain, $z_{\text{C}}[m,n]$ is the additive white Gaussian noise (AWGN) noise with zero mean and variance σ_{z}^2, i.e., $\mathcal{N}_{\mathcal{C}}(0, \sigma_{\text{z}}^2)$. The signal-to-noise ratio (SNR) of the received communication signal at the recipient vehicle is defined as $\zeta_{\text{C}} \triangleq \mathcal{E}_{\text{s}}|h_{\text{C}}|^2/\sigma_{\text{z}}^2$.

Radar Received Signal Model: The radar channel corresponding to the target/recipient vehicle is characterized by its channel gain β_0 at the range bin ℓ_0 that satisfies $\ell_0 T_{\text{s}} - T_{\text{s}}/2 \leq 2\rho_0/c \leq \ell_0 T_{\text{s}} + T_{\text{s}}/2$ with c as the speed of light, and Doppler shift $\nu_0 \triangleq 2v_0/\lambda$, where λ is the wavelength. Assuming perfect interference cancellation of the data part on the received preamble, the discrete-time received radar signal corresponding to the P symbol preamble of m^{th} frame located at $q_m T_{\text{s}}$ can be expressed as

$$y_m[n] = \beta_0 \mathrm{e}^{\mathrm{j}2\pi\nu_0 q_m T_{\text{s}}} s[n - \ell_0] + z_{\text{R}}[m,n] \tag{3}$$

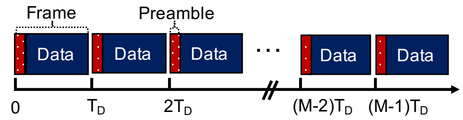

Fig. 2. Uniform pulse approach, where a CPI consists of M equispaced frames of T_{D} duration. Here, each frame contains fixed preamble and data lengths.

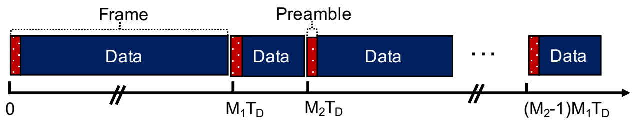

Fig. 3. Virtual pulse approach, where a CPI consists of non-uniformly placed $M = M_1 + M_2$ frames. Here, each frame consists of a fixed preamble length and a varying data length.

where $s[n - \ell_0] = s_m[n - \ell_0]$ is the preamble part of m^{th} frame that remains the same for each frame. The noise term $z_{\text{R}}[m,n]$ is assumed to be Gaussian distributed as $\mathcal{N}_{\mathcal{C}}(0, \sigma_{\text{z}}^2)$ and it is uncorrelated with β_0.

3. UNIFORM AND VIRTUAL PULSES

In this section, we describe the uniform and virtual pulse design approaches for the adaptive IEEE 802.11ad-based joint system along with their associated processing algorithms.

Frame Structure: The frames can be placed either with a constant distance between them, as shown in Fig. 2 or with varying distance, as shown in Fig. 3. In either case, the location of m^{th} frame is assumed to be $p_m T_{\text{D}}$, where p_m is a positive integer and $T_{\text{D}} \triangleq 1/(2\nu_{\max})$ is the Nyquist sampling interval with maximum relative Doppler shift $\nu_{\max}$. Both the pulse approaches use a fixed IEEE 802.11ad preamble with 3328 symbols. For the uniform pulse approach in [3], the number of symbols per frame, N_m, is constant and $N_m T_{\text{s}} = T_{\text{D}}$ meets the Nyquist criterion, while for the virtual pulse approach, N_m is varying and chosen in a sub-Nyquist fashion such that $N_m T_{\text{s}} \geq T_{\text{D}}$. The virtual pulse approach is conceptually similar to the concepts of staggered pulse repetition intervals (PRI) used in the classical long range radar [11, Ch. 17] and sparse sampling/arrays used in the undersampled frequency/angle/channel estimation [12–14]. For tractable analysis, we specifically use here the coprime approach [13] for optimally selecting the locations, $\{p_m\}_{m=1}^{M}$, and the number of frames, M, in a given CPI.

Let $\{M_k\}_{k=1}^{K}$ denote a set of K positive integers which are relatively coprime. Also assume without loss of generality that $M_k < M_{k+1}$. Then K data blocks, each consisting of M_k uniformly spaced undersampled frames, need to be placed according to the coprime approach [13]. For example, for a single coprime pair $\{M_1, M_2\}$, the preamble/ is repeated M_1 times with $M_2 T_{\text{D}}$ spacing and then M_2 times with $M_1 T_{\text{D}}$ spacing, as shown in Fig. 3.

Proposed Radar Processing: We now describe a generic radar processing for target velocity estimation. They exploit the channel estimates derived from the channel estimation field of the IEEE 802.11ad preamble that consists of Golay complementary pair with good auto-correlation properties [3]. The channel corresponding to the detected target in ℓ_0^{th} range bin using m^{th} frame with the correlation integration gain γ, $b_0 \triangleq \gamma\sqrt{\mathcal{E}_{\text{s}}}\beta_0$, and $u_0 \triangleq \nu_0 T_{\text{D}}$ is

$$\hat{h}_m[\ell_0] = b_0 \mathrm{e}^{\mathrm{j}2\pi u_0 p_m} + z_m[\ell_0] \tag{4}$$

where the noise $z_m[\ell_0]$ is distributed as $\mathcal{N}_{\mathcal{C}}(0, \sigma_{\text{z}}^2)$. The SNR of the estimated radar channel is defined as $\zeta_{\text{R}}[\ell_0] \triangleq b_0^2/\sigma_{\text{z}}^2$. The estimated channel vector for a CPI of M frames is $\mathbf{h}[\ell_0] \triangleq \left[\hat{h}_0[\ell_0], \cdots, \hat{h}_{M-1}[\ell_0]\right]^T$ and is given by

$$\mathbf{h}[\ell_0] = \mathbf{d}(v_0) b_0 + \mathbf{z}[\ell_0] \tag{5}$$

where $\mathbf{d}(v_0) \triangleq [1, e^{j2\pi u_0 p_1}, \cdots, e^{j2\pi u_0 p_{M-1}}]^T$ is the velocity vector and $\mathbf{z}[\ell_0]$ denotes the noise vector.

Due to the space limitation and for simplicity of our showcase study here, we consider only the FFT-based velocity estimation algorithm for the uniform pulse design approach and the analogous Chinese remainder theorem (CRT)-based algorithm for the virtual pulse design approach, among many possible [13, 15]. The FFT-based technique has been used in the classical radar processing and the CRT-based technique in coprime pulsing for resolving range/Doppler ambiguities in a long range scenario [11, Ch. 17].

For the uniform approach, the velocity estimated from (5) using FFT requires long radar pulse integration with a large number of uniformly placed preambles to achieve high velocity estimation accuracy/resolution. The physical increase in the number of radar pulses during a CPI, however, significantly reduces the communication spectral efficiency.

The velocity estimation performance can be significantly improved without decreasing communication rate much within a CPI by placing a few radar pulses in a coprime fashion to construct a virtual block with larger number of pulses. The velocity estimation algorithm for the virtual approach make use of CRT on the K detected peak locations that are obtained from the FFTs over the $\{M_k\}_{k=1}^K$ uniformly spaced undersampled pulses. In particular for a coprime pair $\{M_1, M_2\}$, the peak location pair, $\{\eta_1, \eta_2\}$, is obtained from the FFTs of the M_1 and M_2 uniformly spaced undersampled pulses with $0 \leq \eta_1 \leq M_1 - 1$ and $0 \leq \eta_2 \leq M_2 - 1$. Then, a unique i in the range of $0 \leq i \leq M_1 M_2$ satisfying $i = M_1 m_2 + \eta_1 = M_2 m_1 + \eta_2$ is estimated using the CRT. Therefore, we get the effect of $M_1 M_2$ uniformly placed pulses at the Nyquist rate by only using $M_1 + M_2 - 1$ coprime pulses at the sub-Nyquist rate. This approach can be extended to a multi-target robust scenario using modified CRT [16, 17].

4. SPARSITY-AWARE WAVEFORM DESIGN

The radar performance for the FFT-based uniform pulse design approach and the CRT-based virtual pulse design approach is evaluated based on the velocity estimation accuracy/resolution metric. The velocity resolution is defined as

$$\Delta_{\text{v}} \triangleq \frac{\lambda}{2 M_{\text{I}} T_{\text{D}}} \tag{6}$$

where M_{I} indicates the identifiablity for the velocity estimation, which is M for the uniform pulse approach and $\prod_{k=1}^K M_k$ for the virtual pulse approach. The velocity estimation accuracy is defined as the mean absolute error (MAE), i.e., $\text{MAE}_{\text{v}} \triangleq \mathbb{E}[|\hat{v} - v|]$, where $\hat{v}$ is the estimated velocity and v is the true velocity. For high radar SNR, $\text{MAE}_{\text{v}} \leq \Delta_{\text{v}}$.

The communication performance for the joint system is evaluated using the rate-distortion metric defined as [18]

$$\Delta_{\text{C}} \triangleq 2^{-r_{\text{eff}}} = \frac{1}{(1 + \zeta_{\text{C}})^{\chi}} \tag{7}$$

where $r_{\text{eff}} \triangleq \chi \log_2(1 + \zeta_{\text{C}})$ is the effective spectral efficiency and χ is the fraction of communication data symbols in a CPI. Specifically, in the case of uniform pulses, $\chi \triangleq M\left(PT_{\text{s}} + T_{\text{IFS}}\right)/T$ where T_{IFS} is the interframe spacing, while in the case of virtual pulses, $\chi \triangleq \left(\sum_{k=1}^K M_k - 1\right)\left(PT_{\text{s}} + T_{\text{IFS}}\right)/T$.

The joint communication-radar performance optimization is a multi-objective problem of simultaneously optimizing both the radar performance, in terms of, for example, improving Δ_{v} and communication performance, in terms of minimizing Δ_{C}. Using the scalarization approach known to achieve a Pareto optimal point for multiple objectives, if they are convex, the joint optimization can be formulated as

$$\begin{aligned} \underset{\{M_k\}_{k=1}^K}{\text{minimize}} \quad & \omega_{\text{R}} \log \Delta_{\text{v}} + \omega_{\text{C}} \log \Delta_{\text{C}} \\ \text{subject to} \quad & 0 < M_k < M_{k+1} \end{aligned} \tag{8}$$

where ω_{R} and ω_{C} are the positive normalizing and weighting factors assigning the priorities for radar and communication tasks, which can be adjusted adaptively to meet the requirements imposed by different vehicular scenarios. For example, the weights can be assigned to ensure proportional fairness between two objectives. Alternatively, problem (8) can be modified as minimization of one of the objectives with second as a constraint that would guarantee an acceptable performance for one of the tasks. It has been demonstrated in [19] that the valid optimal coprime pair under some mild conditions is obtained when M_2 and M_1 is as close as possible, for example, $M_2 = M_1 + 1$. For this coprime pair, (8) is convex and can be solved efficiently. Finally, it is worth to note that the radar performance metric in (8) can also be replaced by MAE_{v}, mean square error, or Cramer-Rao bound (CRB). The latter two we skip here because of the space limitation.

5. SIMULATION RESULTS

The trade-off between radar and communication performances for the proposed virtual pulse approach and the

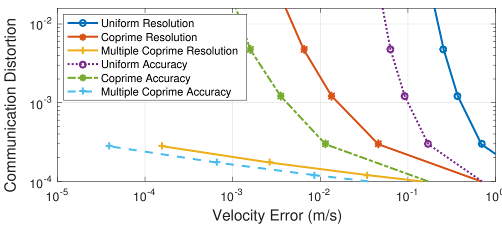

(a) Trade-off at $\rho_0 = 10$ m

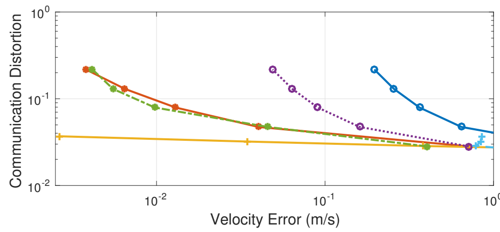

(b) Trade-off at $\rho_0 = 100$ m

Fig. 4. Trade-off between radar velocity accuracy/resolution and communication distortion for different distances.

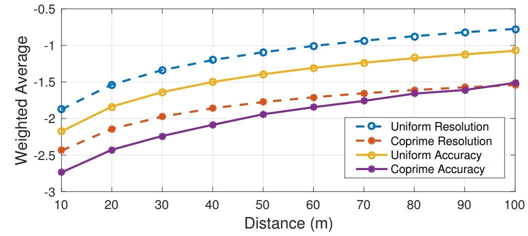

(a) Optimized weighted average increases with distance

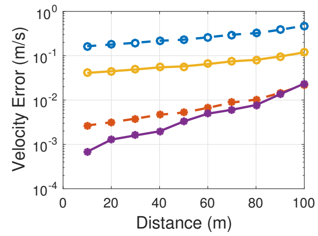

(b) Velocity error increases with distance

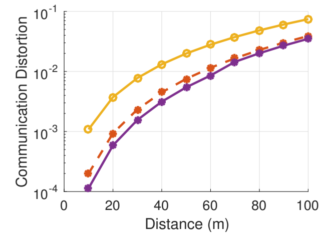

(c) Rate-distortion increases with distance

Fig. 5. Optimized velocity estimation accuracy/resolution and communication rate-distortion with varying distances.

uniform pulse approach in [3] is investigated by means of simulations. Two virtual pulse approaches are explored with $5 \leq M \leq 100$: one is based on a single coprime pair $M_2 = M_1 + 1$, while another makes use of multiple coprime pairs that allows minimum trade-off with the communication rate-distortion at high SNR. We assume a radar cross section of 10 dBsm [20] and a CPI of 1 ms, which is less than the typically used CPI [21, Ch. 7]. In simulations, v_0 is varied uniformly from 0 to 20 m/s and ρ_0 from 10 to 100 m, which falls within typical automotive radar specifications [22, 23].

Figs. 4(a) and (b) demonstrate the trade-off between velocity estimation accuracy/resolution and communication rate-distortion for ρ_0 of 10 m and 100 m, respectively. The coprime structure significantly relaxes the trade-off compared to the uniform structure. At smaller distances, multiple coprime approach works the best, followed by a single coprime pair. As the distance increases, the gap between the coprime and uniform approach decreases and the multiple coprime approach degrades much faster as compared to the single coprime pair. Therefore, we compare a single coprime approach with the uniform approach for joint waveform design.

Fig. 5 shows the joint performance of the waveform designs tested versus $\rho_0 \leq 100$ m. Specifically, Fig. 5(a) shows the optimized weighted average of Δ_C and radar velocity estimation resolution/MAE with equal weighting, while Fig. 5(b) shows the optimized target velocity accuracy/resolution for a required $\Delta_C = 0.0635$, which corresponds to 7 Gbps data rate. At $\rho_0 = 10$ m, the velocity resolution and MAE is improved by a factor of 61.5 and 60.5, respectively. At $\rho_0 = 100$ m, the velocity resolution and MAE is improved by a factor of 21.5 and 5, respectively. Fig. 5(c) shows the optimized Δ_C for a required 1 cm/s velocity accuracy. At $\rho_0 = 10$ m, Δ_C using coprime pulse approach has improved 9.6 times over the uniform pulse approach, while at $\rho_0 = 100$ m, the improvement is only 2.1 times. The uniform pulse approach does not meet the required cm/s-level velocity resolution in a 1 ms CPI, whereas the virtual pulse approach achieves this resolution with lower than 0.04 rate-distortion. Figs. 5(a)–(c) show that as the vehicle separation distance grows, the velocity MAE increases, moves closer to the coprime velocity resolution, and the improvement over the uniform pulse-based design decreases. The velocity MAE of uniform/virtual pulses decrease with distance due to the reduction in SNR, while the advantage of virtual pulses over the uniform pulses decreases due to the poor performance of the CRT at lower SNR.

6. CONCLUSION

A virtual pulse design approach for IEEE 802.11ad-based joint communication-radar is developed by non-uniformly placing the preambles in a CPI. For tractability and simplicity, we chose a coprime-based approach and the CRT for virtually constructing higher number of pulses. The trade-off between the communication and radar performance is optimized by formulating a scalarized joint metric of communication rate-distortion and radar velocity estimation accuracy/resolution. Numerical results demonstrate that the coprime-based pulse design approach significantly improves the velocity estimation accuracy/resolution for a required communication rate-distortion as well as it improves the optimized weighted average of the two conflicting metrics, as compared to the uniform pulse design approach. Specifically for the CRT-based algorithm, the factor of improvement increases with the decreasing vehicle separation distance. This work can be extended by considering other sparse array structures, robust processing algorithms, and other radar performance metrics.

7. REFERENCES

[1] L. Han and K. Wu, "Joint wireless communication and radar sensing systems–state of the art and future prospects," *IET Microwaves, Antennas & Propagation*, vol. 7, no. 11, pp. 876–885, 2013.

[2] P. Kumari, N. Gonzalez-Prelcic, and R. W. Heath Jr, "Investigating the IEEE 802.11ad Standard for Millimeter Wave Automotive Radar," in *Proceedings of the 82nd IEEE Vehicular Technology Conference*, Sept 2015, pp. 3587–3591.

[3] P. Kumari, J. Choi, N. Gonzalez-Prelcic, and R. W. Heath Jr, "IEEE 802.11ad-based Radar: An Approach to Joint Vehicular Communication-Radar System," *Accepted to IEEE Transactions on Vehicular Technology*, Oct 2017.

[4] J. Hasch, E. Topak, R. Schnabel, T. Zwick, R. Weigel, and C. Waldschmidt, "Millimeter-wave technology for automotive radar sensors in the 77 GHz frequency band," *IEEE Transactions on Microwave Theory and Techniques*, vol. 60, no. 3, pp. 845–860, 2012.

[5] N. A. Estep, D. L. Sounas, J. Soric, and A. Alù, "Magnetic-free non-reciprocity and isolation based on parametrically modulated coupled-resonator loops," *Nature Physics*, vol. 10, no. 12, pp. 923–927, 2014.

[6] Z. Xiao, P. Xia, and X. G. Xia, "Full-duplex millimeter-wave communication," *IEEE Wireless Communications*, vol. 24, no. 6, pp. 136–143, Dec 2017.

[7] V. Va, T. Shimizu, G. Bansal, and R. W. Heath Jr, "Millimeter wave vehicular communications: A survey," *Now: Foundations and Trends in Networking*, vol. 10, no. 1, 2016.

[8] A. Bazzi, C. Kärnfelt, A. Peden, T. Chonavel, P. Galaup, and F. Bodereau, "Estimation techniques and simulation platforms for 77 GHz FMCW ACC radars," *The European Physical Journal Applied Physics*, vol. 57, no. 01, p. 11001, 2012.

[9] J. Kim and A. F. Molisch, "Enabling gigabit services for IEEE 802.11 ad-capable high-speed train networks," in *IEEE Radio and Wireless Symposium (RWS)*, 2013, pp. 145–147.

[10] T. S. Rappaport, G. R. MacCartney, M. K. Samimi, and S. Sun, "Wideband millimeter-wave propagation measurements and channel models for future wireless communication system design," *IEEE Transactions on Communications*, vol. 63, no. 9, pp. 3029–3056, Sept 2015.

[11] M. I. Skolnik, Ed., *Radar Handbook*, 2nd ed. McGraw Hill, 1990.

[12] A. Moffet, "Minimum-redundancy linear arrays," *IEEE Transactions on Antennas and Propagation*, vol. 16, no. 2, pp. 172–175, Mar 1968.

[13] P. P. Vaidyanathan and P. Pal, "Sparse sensing with co-prime samplers and arrays," *IEEE Transactions on Signal Processing*, vol. 59, no. 2, pp. 573–586, Feb 2011.

[14] K. V. Mishra and Y. C. Eldar, "Sub-Nyquist channel estimation over IEEE 802.11ad link," in *Proceedings of the International Conference on Sampling Theory and Applications (SampTA)*, July 2017, pp. 355–359.

[15] P. Stoica and R. L. Moses, *Spectral analysis of signals*. Upper Saddle River, NJ: Prentice-Hall, 2005.

[16] X.-G. Xia, "On estimation of multiple frequencies in undersampled complex valued waveforms," *IEEE Transactions on Signal Processing*, vol. 47, no. 12, pp. 3417–3419, Dec 1999.

[17] X.-G. Xia and K. Liu, "A generalized Chinese remainder theorem for residue sets with errors and its application in frequency determination from multiple sensors with low sampling rates," *IEEE Signal Processing Letters*, vol. 12, no. 11, pp. 768–771, Nov 2005.

[18] P. Kumari, D. H. N. Nguyen, and R. W. Heath, "Performance trade-off in an adaptive IEEE 802.11ad waveform design for a joint automotive radar and communication system," in *Proceedings of the International Conference on Acoustics, Speech and Signal Processing (ICASSP)*, Mar 2017, pp. 4281–4285.

[19] K. Adhikari, J. R. Buck, and K. E. Wage, "Extending coprime sensor arrays to achieve the peak side lobe height of a full uniform linear array," *EURASIP Journal on Advances in Signal Processing*, vol. 2014, no. 1, p. 148, Sep 2014. [Online]. Available: https://doi.org/10.1186/1687-6180-2014-148

[20] "Intelligent transport systems – adaptive cruise control systems – performance requirements and test procedures," *ISO 15622:2010*, 2010.

[21] F. Gini, A. De Maio, and L. Patton, *Waveform design and diversity for advanced radar systems*. The Institution of Engineering and Technology, 2012.

[22] M. Murad, I. Bilik, M. Friesen, J. Nickolaou, J. Salinger, K. Geary, and J. S. Colburn, "Requirements for next generation automotive radars," in *2013 IEEE Radar Conference (RadarCon13)*, April 2013, pp. 1–6.

[23] S. M. Patole, M. Torlak, D. Wang, and M. Ali, "Automotive radars: A review of signal processing techniques," *IEEE Signal Processing Magazine*, vol. 34, no. 2, pp. 22–35, March 2017.